The melting of glucose

Jean-François Willart, S. Ouerghemmi, N. Descamps, P. Heijboer, Laurent
Paccou, Florence Danede, Marc Descamps

The melting of glucose

J.F. Willart[1], S. Ouerghemmi[1], N. Descamps[2], P. Heijboer[2]
L. Paccou[1], F. Danède[1], M. Descamps[1]

[1] Univ. Lille, CNRS, INRAE, Centrale Lille, UMR 8207
UMET - Unité Matériaux et Transformations F-59000 Lille, France

[2] Roquette Frères, 10 rue haute loge, F-62136 Lestrem, France

Corresponding author: Jean-Francois.Willart@univ-lille.fr

Abstract

Several sugars are known to undergo a spontaneous liquefaction below their reputed melting point (T_m), but the origin of this apparent melting is not yet clearly understood. In this paper we address this puzzling behavior in the particular case of the crystalline forms of glucose : $G\alpha$ and $G\beta$, involving respectively the glucose-α and glucose-β anomers. We show in particular that the spontaneous melting below their reputed melting point T_m (~151°C for $G\alpha$ and ~156°C for $G\beta$) corresponds to a horizontal displacement of the system in the eutectic phase diagram of the anomeric mixture glucose-α / glucose-β. This displacement is associated with mutarotation in the liquid which, in turn, induces additional liquefaction of the remaining crystal. This feedback loop creates a vicious circle which stops when the mixture reaches the liquidus branch, i.e. when the liquefaction is total. It is also shown that this behavior becomes more complex on approaching the eutectic temperature T_e (120°C). Just above T_e, the liquefaction process is followed by a recrystallization leading to the crystalline form $G\beta$. On the other hand, just below T_e, the spontaneous liquefaction process stops as no melting is expected whatever the anomeric composition.

1. INTRODUCTION

Sugars are widely used as excipients in the pharmaceutical industry because they combine many advantages for the formulation of drugs. In particular, they can facilitate compacting of tablets, improve the dissolution properties of drugs, increase the physical and chemical stability of drugs during storage, protect labile active biomolecules from processing stresses[1-5] (freeze drying and spray drying for example) and mask unpleasant tastes. Given their great use, most sugars (glucose, fructose, sucrose, lactose, trehalose…) have been extensively studied and their main physical and chemical properties are very well characterized[6,7].

However, several sugars (glucose, fructose, galactose…) have been reported to show very unusual melting properties, the origin of which is not yet clearly established. For instance, several papers report a strong dependence of the melting temperature of these sugars on the heating rate[8-13]. As shown in table 1, adiabatic calorimetry, DSC and hyper DSC measurements have revealed that the melting point of fructose increases from 89 to 136°C for heating rates ranging from 0.01°C/min to 1500°C/min. In the case of glucose (table 2), the melting point was found to shift from 140°C to 183°C for heating rates ranging from 0.05°C/min to 1500°C/min. Tombari et al. have also shown that crystalline fructose undergoes a spontaneous liquefaction during isothermal treatments at temperatures well below its "reputed" melting point (105°C)[13] determined through classical DSC experiments. For example, complete liquefaction takes place, in one day at 90°C. Similar liquefaction processes below their reputed melting point have also been noted for several other sugars such as glucose[13] and galactose[13]. While impressive and of prime interest, the mechanisms which drive these unexpected liquefaction processes remain an open question.

Up to now, three scenarios have mainly been proposed to explain the dependence of the melting temperature on the heating rate:

The first one, proposes that some sugars can be easily superheated due to slow melting kinetics, so that the higher the heating rate the higher their apparent melting point[9,10,14]. In that case, the true melting temperature would be obtained for very low heating rates. Magon et al. studied the evolution of the melting temperature of fructose[10] and glucose[9] for decreasing heating rates. Extrapolation to zero heating rate of their results predicts a melting temperature of fructose close to 97°C and a melting temperature of glucose close to 140°C. However, these findings are not compatible with those of Tombari et al.[13] which show that fructose and glucose liquefy in a few hours when annealed below these extrapolated melting points. For instance, complete liquefaction of fructose is found to occur within 140 hours upon annealing at 85°C and that of glucose is completed within 6 hours upon annealing at 135°C.

The second scenario supposes that some fast thermal decomposition occurs upon heating, before reaching the melting point. Decomposition products would then act as impurities, leading to a decrease of the apparent melting temperature[15,16]. Lee et al.[16] called "apparent melting" this loss of crystalline order due to chemical decomposition. In these conditions - and contrary to the first scenario - the true melting point of sugars would thus be obtained for high heating rates which limit thermal decompositions before melting. Hyper DSC experiments conducted by Lee et al.[11] have shown that the maximum melting temperature of fructose is 136°C for a heating rate of 1500°C / min (For comparison, this temperature is 115°C at 20°C / min). However, the "apparent melting" scenario was refuted by Roos et al. in a very useful clarification paper[12]. These authors have shown that thermal decomposition does not occur on crystals surface but occur in the liquid phase produced by the melting. Decomposition thus appears to be more a consequence of the melting rather than a cause.

A third scenario was proposed by Tombari et al.[13] who noticed that these non-conventional melting mainly concerns isomerizable sugars and postulated that isomeric conversions of sugar molecules can occur in the crystal. The molecular

structure of the new anomer is expected to be incompatible with both the existing crystal lattice and the network of hydrogen bonds, creating an amorphous zone which cannot recrystallize. This isomerization within the crystal would be allowed and facilitated by the crystal defects (vacancies and dislocations). Their random diffusion, would then make it possible to progressively amorphize the whole sample. Under these conditions the true melting point of the "pure" isomer would thus be obtained for high heating rates which limit the isomerization process before melting. Tombari et al. have investigated in details the isothermal melting kinetic of fructose far below its reputed melting point. The temperature dependence of the characteristic liquefaction time has been found to be arrhenian suggesting that isothermal melting of fructose could occur at any temperature and even at room temperature where the half liquefaction time was estimated at 74200 years.

In this paper, we show that the liquefaction of glucose α (Gα) and glucose β (Gβ) below their reputed melting points is directly induced by a coupling between liquefaction and mutarotation. It is shown to be driven by the necessity to accommodate the physical and chemical equilibrium states of the system in the eutectic phase diagram of the glucose-α/glucose-β binary mixture[17]. This mechanism also suggests that the liquefaction process move to a recrystallisation process toward Gβ in a small temperature range located just above the eutectic temperature. Several experimental proofs of this unexpected recrystallization are presented which reinforces the validity of the proposed liquefaction mechanism. The whole investigation leads us to propose a universal mechanism able to explain the rich pattern of evolutions of glucose below T_m and potentially in any other isomerizable sugar.

2. EXPERIMENTALS

Glucose α (Gα) was provided by Roquette (Lestrem, France) (Dextrose Anhydrous C ®, purity 99.5 %) and **Glucose β (Gβ)** was purchased from Cayman Chemical (purity 98.0%). Powder X-ray diffraction analysis have shown that the two compounds have crystalline structures (space group $P2_12_12_1$) identical to those determined by McDonald et Beevers[18] for Gα and Chu and Jeffrey[19] for Gβ. Before use, both materials were systematically annealed during one hour à 70°C to remove any residual free water. PXRD and NMR experiments have shown that this drying stage has no effect on both the structural state and the anomeric composition of the materials. Samples were then immediately subjected to specific thermal treatments at high temperature (above 100°C) preventing any subsequent absorption of water during their study.

Differential Scanning Calorimetry (DSC) experiments were performed with a Q200 calorimeter of TA Instruments (Guyancourt, France). During all the measurements the calorimeter head was flushed with highly pure nitrogen gas. Temperature and enthalpy readings were calibrated using pure indium at the same scan rates used in the experiments. All scans were performed in the temperature modulated mode (MDSC) using an average heating rate of 5°C/min, a modulation amplitude of 0.663°C and a modulation period of 50 sec. Samples were placed in hermetic aluminum pans.

Isothermal calorimetry experiments were performed with a microcalorimeter MicroDSC7 evo of Setaram (Caluire, France). The samples (200 mg) were placed into hermetic hastelloy cells which were then introduced directly in the calorimeter previously equilibrated at the desired annealing temperature. This protocol allows to skip the slow heating stage from the RT to the annealing temperature and thus limits, as much as possible, any potential chemical and structural evolutions which could occur before the annealing stage.

Powder X-Ray Diffraction (PXRD) experiments were performed with a PanAlytical X'PERT PRO MPD (Almelo, The Netherlands) diffractometer (λCuK_α = 1.5418 Å for combined $K_\alpha 1$ and $K_\alpha 2$), equipped with an X'celerator detector (Almelo, The Netherlands) allowing acquisition of diffraction patterns from 2θ= 4° to 2θ= 60° with a scan step of 0.0167 °/s. Samples were placed into aluminum plates (13 mm diameter and 2 mm depth) installed on a rotating (15 rpm) sample holder to avoid artifacts due to preferential orientations of crystallites. No baseline correction was made on the recorded PXRD data.

NMR spectra were recorded with the NMR 400 MHz spectrometer from Bruker (Rheinstetten, Germany). 10 mg of sample were dissolved into 0.75ml of dimethyl sulfoxide (DMSO). This solvent was used for its ability to strongly slow down the mutarotation in solution. The spectra were recorded at RT just after (typically 3 min) the dissolution, in order to limit as much as possible mutarotation. For all experiments we used a 5 mm TBI probe which is suitable for proton NMR. Results were analyzed using the TopSpin 3.5pl5 software of Bruker.

Long isothermal annealing (2 years) at 120°C were performed in a CrystalBreeder (Technobis, Alkmaar, The Netherland) which is able to maintain this temperature within 0.1°C during years.

3. RESULTS

α-D-glucopyranose (α-glucose) and β-D-glucopyranose (β-glucose) are two anomeric forms of the glucose molecule ($C_6H_{12}O_6$) which differ by the orientation of the OH group linked to the C1 carbon. α-glucose and β-glucose crystallize respectively in the forms $G\alpha$[18,20] (space group $P2_12_12_1$) and $G\beta$[19,21] (space group $P2_12_12_1$). Figure 1 shows the heating DSC scans of $G\alpha$ and $G\beta$ recorded at 5°C/min. They both show a well-defined endothermic pic signaling the melting of the materials at respectively T_m^{α} = 151°C and T_m^{β} = 156°C. These values are coherent with those reported in the literature for similar heating rates. However, T_m^{α} and T_m^{β} will be called here "apparent melting temperatures" as the melting point of glucose is known to be very dependent on the heating rate[8-13]. The associated melting enthalpies are respectively: ΔH_m^{α} = 191 J/g and ΔH_m^{β} = 160 J/g.

The structural evolutions of $G\alpha$ and $G\beta$ upon isothermal annealing below their apparent melting point (T_m^{α} = 151°C and T_m^{β} = 156°C respectively) were investigated by isothermal microcalorimetry. The annealing were performed at different temperatures ranging from 131.6 to 143.7°C for $G\alpha$ and from 133.5 to 144.3°C for $G\beta$. The time evolutions of the heat flow recorded during the annealing are reported in figures 2a and 3a in a log scale. They all show an endothermic peak corresponding to the liquefaction of the samples. The corresponding enthalpies are those expected for the melting enthalpies of $G\alpha$ (~191 J/g) and $G\beta$ (~160 J/g) indicating that the liquefaction is complete after each annealing. The running integral of the heat flow curves normalized to 1 then gives directly access to the kinetics of the liquefaction process at each annealing temperature as reported in figures 2b and 3b in a log scale. It appears that the lower the annealing temperature the slower the liquefaction process. The Arrhenius plot of figure 4 shows the evolution of the half liquefaction time ($t_{1/2}$) against the annealing temperature. This evolution is linear which reveals the Arrhenius character of the liquefaction process similar to that found by Tombari[13] et al. for

fructose. This could suggest that the liquefaction process slows down at lower temperatures but never stops. We will show below that it is in fact not the case.

The tautomeric evolutions of $G\alpha$ and $G\beta$ samples during annealing below T_m have been investigated by NMR. Crystalline samples of $G\alpha$ and $G\beta$ (10 mg) were annealed respectively at 140 ° C and 145 ° C for annealing times varying from 0 to 10 h. The samples were then dissolved in 75 ml of DMSO (dimethyl sulfoxide) and immediately analyzed by liquid NMR to determine their tautomeric composition. The details of the measurement protocol and its validity are presented in the supplementary data. The NMR spectra of annealed $G\alpha$ and $G\beta$ samples reveal a striking evolution of the anomeric composition of the two materials. These evolutions are reported respectively in figure 5a and 5b. We can note the development of the anomer β in the $G\alpha$ sample and the development of the anomer α in the $G\beta$ sample. Moreover, the α and β anomer fractions (respectively X_α and X_β) in both samples tend toward those of amorphous glucose obtained by melt-quenching[22] ($X_\alpha = 0.44$ and $X_\beta = 0.56$). These experiments thus show that the isothermal amorphization of glucose below its "apparent melting temperature" is accompanied by a strong mutarotation. This conclusion agrees with the hypothesis of Tombari et al.[13] who proposed that the isothermal liquefaction of anomerizable sugars could be due to a slow mutarotation in the crystalline state. However, the present results indicate that the time required to reach the anomeric equilibrium (10h for $G\alpha$ at 140°C and 6h for $G\beta$ at 145°C) is significantly longer than the liquefaction completion time (about 4h for $G\alpha$ at 140°C and 3h for $G\beta$ at 145 °C, figures 2 and 3). This indicates that the anomeric conversion occurs during the entire amorphization stage and then continues in the liquid state. It also suggests that mutarotation mainly occurs in the liquid state rather than in the crystalline state.

4. DISCUSSION AND COMPLEMENTARY ANALYSIS

Recently, Dujardin et al. determined the phase diagram of the anomeric mixture glucose-α / glucose-β by taking advantage of the amorphization capability of high energy mechanical milling[17]. This solid state amorphization route does not induce any mutarotation and makes it possible to obtain alloys of glucose-α and glucose-β of controlled anomeric composition. As sketched in figure 6, the phase diagram appears to be a simple eutectic phase diagram with an eutectic concentration close to $X_{\alpha,e}$ = 0.7 and an eutectic temperature around T_e = 120°C. It must also be noted that mutarotation was found to be unavoidable upon melting[22], leading to a liquid mixture of the two anomers. Broido et al.[22] showed that the fractions of anomers α and β in the melt are closed to $X_\alpha(liq)$ = 0.44 and $X_\beta(liq)$ = 0.56. This anomeric equilibrium in the liquid is marked by the dashed vertical line in the phase diagram of figure 6. Interestingly, this line crosses the liquidus line associated with Gβ at a temperature T_x which will be shown below to play a key role in the transformations of Gα and Gβ upon annealing below their melting point.

The investigations presented in section 3 have revealed a strong evolution of the anomeric composition of glucose, during isothermal annealing below the apparent T_m. This change in the anomeric composition corresponds to a horizontal displacement of the point representative of the material in the eutectic phase diagram associated with the anomeric mixture glucose-α / glucose-β. Such a displacement in the eutectic phase diagram is expected to induce different structural transformations of Gα and Gβ depending on the annealing temperature.

4.1 Annealing between T_m and T_x

The horizontal displacements of the points representative of Gα and Gβ in the eutectic phase diagram for annealing temperatures between T_m and T_x are schematized in

figure 6 (trajectories 1 and 2). As a result, the material is expected to liquefy progressively according to its position (temperature / composition) in the phase diagram. The liquefaction is complete when the system reaches the liquidus line. The change in the anomeric composition which results in the displacement of the system in the phase diagram is due to the liquefaction itself and to the subsequent mutarotation in the appearing liquid. Indeed, immediately after liquefaction, the liquid is expected to have an anomeric composition given by the liquidus line at the annealing temperature. Mutarotation then drives the liquid to its equilibrium anomeric composition[22] ($X_\alpha = 44\%$ and $X_\beta = 56\%$). This results in an increase of the fraction of the minority anomer (anomer α in Gβ and anomer β in Gα). The progressive liquefaction of glucose upon annealing below T_m can thus be explained by the combination of two mechanisms of transformation (a physical one and a chemical one) that fuel mutually to progressively induce the total liquefaction of the material (figure 7):

- The physical transformation, is a partial liquefaction of the sample which drives the system toward the equilibrium structural composition (crystal / liquid solution) corresponding to its current anomeric composition, in agreement with the lever rule of the eutectic diagram.

- The chemical transformation, is a strong mutarotation in the previously generated liquid fraction which maintains the equilibrium anomeric composition in this physical state ($X_\alpha = 0.44$). This chemical change thus further increases the liquefaction propension described in the previous step, creating some kind of vicious circle.

The initial onset of liquefaction is likely to be triggered by some anomeric impurities preexisting in the Gα and Gβ samples. In that case, we can thus expect that using anomerically pure samples of Gα and Gβ should help to avoid the sub-T_m liquefaction process and allow an accurate determination of the genuine melting points of Gα and

Gβ. However, as proposed by Tombari et al.[13], initial anomeric impurities could also arise from a very slight mutarotation in the crystal facilitated by vacancies or other crystalline defects.

4.2 Annealing between T_x and T_e

For annealing between T_x and T_e, the same mechanism of physical and chemical transformations is expected. However, contrary to the previous temperature range, the liquidus lines of both Gα and Gβ are in that case on the right-hand side of the vertical line corresponding to the α concentration in the equilibrium liquid ($X\alpha$(liq) = 0.44). This striking difference is expected to have a strong repercussion on the nature of the transformation undergone by Gα and Gβ between T_x and T_e.

4.2.1 In the case of Gβ, any liquid fraction directly produced by the liquefaction mechanism will be characterized by a fraction of anomer α larger than that characterizing the equilibrium liquid ($X\alpha$(liq)=0.44). The equilibration of the anomeric composition of the liquefied fraction by mutarotation will then result in a decrease of $X\alpha$. In the frame of the eutectic phase diagram, such a decrease of $X\alpha$ is expected to induce a crystallization toward Gβ. As a result, Gβ has no liquefaction tendency between T_x and T_e. An anomeric purification of the material could even be expected.

4.2.2 In the case of Gα, any liquefaction followed by mutarotation is also expected to result in a decrease of $X\alpha$ which induces, contrary to Gβ, further liquefaction. This vicious circle is identical to that occurring during annealing between T_m(Gα) and T_x (section 4.1) and is expected to induce a total amorphisation of Gα. However, as shown in figure 6 (trajectory 4) the system is expected to cross the liquidus line of Gβ before reaching $X\alpha$(liq)=0.44. This event triggers both the crystallization of Gβ from the liquid, and a conversion of α anomers to β anomers by mutarotation to maintain the equilibrium anomeric composition in the remaining liquid. This mechanism thus

induces further decrease of $X\alpha$ leading to a second vicious circle identical to that presented in section 4.2.1 and which leads to the total conversion of the system to $G\beta$.

The conversion $G\alpha \rightarrow G\beta$ upon annealing between T_x and T_e can hardly be observed experimentally. This is due to the fact that the liquefaction process of $G\alpha$ which precedes the recrystallization stage toward $G\beta$ is very slow below T_x. The extrapolation of the half liquefaction times ($t_{1/2}$) determined for annealing between T_m and T_x (figure 4) indicates that $t_{1/2} \approx 1500h$ at the eutectic temperature ($T_e = 120$ °C) which leads to unreasonable observation times.

To get rid of this limitation and to reveal the conversion $G\alpha \rightarrow G\beta$ between T_e and T_x, we have followed the structural evolution of a physical mixture of $G\alpha$ and $G\beta$ having the eutectic composition, upon annealing between T_m and T_x. Such a mixture is expected to melt within a short time just above T_e. Figure 8 shows the evolution of the X-ray diffraction pattern of the eutectic physical mixture $G\alpha/G\beta$ [75:25] during an annealing at 130°C (ie just above $T_e = 120$°C). The x-ray diffraction patterns of pure $G\alpha$ and pure $G\beta$ recorded at the same temperature (130°C) are also reported for comparison. At t = 0 min, the diffractogram of the eutectic mixture shows the Bragg peaks of both $G\alpha$ and $G\beta$. Upon annealing, we can then observe a progressive decrease of Bragg peaks characteristic of $G\alpha$ in parallel with the development of Bragg peaks characteristic of $G\beta$. This evolution reveals a conversion of $G\alpha$ toward $G\beta$. After 70 min of annealing the Bragg peaks of $G\alpha$ have totally disappeared while those of $G\beta$ stop increasing which indicates that the transformation is complete. Figure 9 compares the heating DSC scan (5°C/min) of the physical mixture recorded after annealing (run 1) to that of the quenched liquid (run2). The annealed sample (run 1) shows a strong and well-defined endotherm corresponding to the melting of $G\beta$ while no sign of glass transition characteristic of the quenched liquid (run 2) could be observed. All these features thus indicate that $G\alpha$ has undergone a total conversion toward $G\beta$ upon annealing just above the eutectic temperature. Such an evolution is in perfect

agreement with that expected by the displacement of the $G\alpha/G\beta$ binary system in its eutectic phase diagram due to the mutarotation in the liquid state. It appears to be a strong validation of the transformation mechanism of glucose below T_m proposed in this paper.

The conversion $G\alpha \rightarrow G\beta$ can also be observed in certain circumstances during heating experiments. This is clearly illustrated in figure 10 which shows heating DSC scans of the physical mixture of $G\alpha$ / $G\beta$ having the eutectic composition ($X_\alpha = 0.75$). Three heating rates have been used: 0.5, 5 and 50°C/min. At 5°C/min the scan only shows a single and well-defined melting peak located at $T_{extra} = 140°C$ defined as the crossing point temperature of the base line and the steepest tangent of the leading edge of the peak. This melting point is much lower than those of pure $G\alpha$ and $G\beta$, and appears to be characteristic of the melting of the eutectic mixture. It must be noted that the onset of melting starts around $T_{onset} = 120°C$ which confirms that the eutectic temperature (T_e) is close to 120°C. At 50°C/min, the melting pic broadens and its maximum shifts toward the high temperatures. These features are merely due to the higher heating rate which makes the time scale of the experiment much shorter than the time scale of melting. However, it must be noted that the melting temperature defined as T_{extra} is unchanged ($T_{extra} = 140°C$) as expected for the melting of an eutectic mixture. Interestingly, at 0.5°C/min, the thermogram is strongly modified. It shows two thin endotherms divided by a small exotherm. These unexpected features can be clearly understood in the frame of the eutectic phase diagram of $G\alpha/G\beta$ in figure 6. The first endotherm corresponds to the melting of the eutectic mixture as the corresponding melting temperature (T_{extra}) is identical to that measured at 5 and 50°C/min. The next exotherm corresponds to the recrystallization of the melt toward $G\beta$. This recrystallization is due to the mutarotation in the melt which drives spontaneously the liquid toward its equilibrium anomeric composition ($X_\alpha = 0.44$[22]). This composition shift involves crossing the liquidus line which leads to a progressive recrystallization of $G\beta$ from the liquid (Inset of figure 10 - black trajectory). These structural and anomeric

evolutions correspond to the trajectory 4 in the diagram of figure 6. Upon further heating, crystalline Gβ progressively liquefies above T_x and disappears definitively when the liquidus is crossed again. This last structural evolution corresponds to the trajectory 1 in the diagram of figure 6. As illustrated in the insert of figure 6, the crossing of the liquidus can only occur if the heating rate is low compared to the mutarotation rate. This is why transient recrystallization occurs at 0.5 ° C / min but does not for higher heating rates (e.g. 5 and 50°C/min). The DSC scans of figure 10 thus show the reality of the eutectic phase diagram of Gα / Gβ mixtures, confirm the eutectic temperature (T_e = 120°C), and give an illustration of the complex structural changes (liquefactions and recrystallization) which can result from the anomeric composition changes due to mutarotation in the liquid phase.

4.3 Annealing below T_e

In the frame of the mechanism proposed in this paper, the liquefaction of glucose is expected <u>to not occur</u> upon annealing below the eutectic temperature (T_e = 120°C) since in this part of the phase diagram, no melting, and thus no mutarotation in the liquid, is expected. To check that point samples of Gα and Gβ were annealed at 120°C during two years inside a Crystal Breeder. The heating (5°C / min) MDSC scans (reversible signal) of the annealed samples are reported in figure 11 and compared to those of the quenched liquids. Clearly, no trace of Cp jump indicative of the glass transitions of Gα and Gβ, can be detected in any of the two samples after this very long annealing. Identical analyzes performed periodically during the annealing have shown exactly the same results. These experiments thus confirm that annealing glucose just below the eutectic temperature of the glucose α / glucose β mixture does not induce any liquefaction of the material. It must be noted that the extrapolation of the Arrhenius behavior of $t_{1/2}$ shown in figure 4 predicts half liquefaction times of 57 days and 147 days at 120°C for Gα and Gβ respectively. These times are significantly less than the duration of the annealing (2 years) which indicates that the absence of

liquefaction at 120°C is not merely due to the extreme slowness of the liquefaction process at this temperature. The liquefaction process thus appears to be really ineffective below the eutectic temperature of the anomeric α/β mixture.

4. CONCLUSION

In this paper, we have identified the origin of the puzzling liquefaction behavior of the two crystalline forms of glucose (Gα and Gβ) upon annealing far below their reputed melting points T_m[13]. This liquefaction was clearly attributed to the displacement of the system in the eutectic diagram of the anomeric α/β binary mixture. Such displacement was shown to result from a feedback loop between liquefaction of the crystalline fraction and mutarotation in the resulting liquid. This loop leads to a continuous enrichment of Gβ (resp. Gα) in anomer α (resp. anomer β) inducing a continuous liquefaction of glucose which becomes total when the system reaches its liquidus line. These transformations are expected to be triggered by preexisting anomeric impurities in the starting crystals.

It was also inferred and then shown, for the first time, that the previous feedback loop can lead to the recrystallization of glucose (whatever its initial anomeric composition) toward Gβ. This behavior is expected to occur between T_e and T_x respectively defined as the eutectic temperature of the anomeric mixture, and the temperature at which the liquidus branch of Gβ has the anomeric composition of the liquid (see figure 6). In this temperature range, the feedback loop liquefaction/mutarotation leads to a continuous enrichment in anomer β for both Gα and Gβ. As a result, no changes are expected for Gβ. On the other hand, the enrichment in anomer β leads to a liquefaction of Gα until its liquidus line is reached, followed by a complete recrystallization toward Gβ once the corresponding liquidus is crossed.

Below T_e, no melting – and thus no mutarotation – is expected in the frame of the eutectic phase diagram. The constant anomeric composition thus leads to stationary physical and chemical states. This point was confirmed through very long annealing (up to 2 years) below T_e during which no trace of liquefaction could be detected.

The feedback loop between liquefaction and mutarotation revealed in this paper was thus shown to be responsible for a rich pattern of structural and chemical transformations of glucose below T_m. These complex mechanisms of transformations are expected to also hold in several other isomerizable sugars (galactose, fructose, lactose, lactulose…). Further investigations are in progress to check their general character.

ACKNOWLEDGEMENTS

CAPTIONS:

Table 1: Typical melting points of fructose reported in the literature for different heating rates ranging from 0.01°C/min to 1500°C/min.

Table 2: Typical melting points of glucose reported in the literature for different heating rates ranging from 0.05°C/min to 1500°C/min.

Figure 1: Heating (5°C/min) DSC scans of Gα and Gβ.

Figure 2: a) Time evolution of the heat flow recorded during the isothermal annealing of Gα at temperatures ranging from 131.6 to 143.7°C. Annealing temperatures are reported above each curve.
b) Amorphization kinetics of Gα during isothermal annealing performed between 131.6 and 143.7°C. These kinetics have been obtained by running integration and normalization of the isothermal heat flow curves of figure 2a.

Figure 3: a) Time evolution of the heat flow recorded during the isothermal annealing of Gβ at temperatures ranging from 133.5 to 144.3°C. Annealing temperatures are reported above each curve.
b) Amorphization kinetics of Gβ during isothermal annealing performed between 133.5 and 144.3°C. These kinetics have been obtained by running integration and normalization of the isothermal heat flow curves of figure 3a.

Figure 4: Arrhenius plot of the half completion time ($t_{1/2}$) characterizing the isothermal liquefaction kinetics of Gα (red circles) and Gβ (blue circles) shown in figures 2b and 3b.

Figure 5: Time evolutions of the anomeric fractions of α-glucose and β-glucose during annealing of Gα and Gβ at 140°C and 145°C respectively.

Figure 6: Schematic eutectic phase diagram of the anomeric α/β binary mixture[17]. The vertical dashed line marks the equilibrium anomeric composition in the liquid state and T_x marks the temperature at which this line crosses the liquidus branch.

The red arrows represent the trajectories of Gα and Gβ in the phase diagram upon annealing above and below T_x :

1: Gβ above T_x (liquefaction)

2: Gα above T_x (liquefaction)

3: Gβ below T_x (no evolution)

4: Gα below T_x (liquefaction and recrystallization toward Gβ)

Figure 7: Schematic illustration of the feedback loops leading to trajectories 1,2, and 4 in the eutectic diagram of the Gα/Gβ mixture shown in figure 6.

Figure 8: X-ray diffraction patterns of the eutectic physical mixture Gα/Gβ [75:25] recorded after different annealing times at 130°C. The annealing times are reported on the left-hand side of each diagram. The X-ray diffraction patterns of Gα and Gβ recorded just after heating at 130°C are also reported for comparison. It must be noted that no evolution of theses X-ray diffraction patterns could be detected in the course of a two-hour annealing at this temperature.

Figure 9: Heating (5°C/min) DSC scans of the eutectic physical mixture Gα/Gβ [75:25] recorded after annealing at 130°C for 80 min (The sample is that obtained at the end of the annealing experiment shown in figure 8). Run 1 corresponds to the first heating and run 2 corresponds to the second one.

Figure 10: DSC scans of the physical mixture Gα/Gβ [75:25] recorded with different
heating rates: 0.5°C/min, 5°C/min and 50°C/min. The insert schematizes
the trajectories of the mixture in the eutectic phase diagram during the three
heating scans.

Figure 11: Heating (5°C/min) DSC scans (reversible signals) of Gα and Gβ recorded
after a two-year annealing at 120°C (black lines). The scans of the
quenched melts are also shown for comparison (green lines).

Table 1

FRUCTOSE			
T_m	Heating rate	Technique	References
89°C	0.01 °C/min	Adiabatic calorimetry	Johari et al. [13]
115°C	20°C /min	DSC	Magon et al. [10]
136°C	1500 °C/min	Hyper DSC	Lee et al. [11]

Table 2

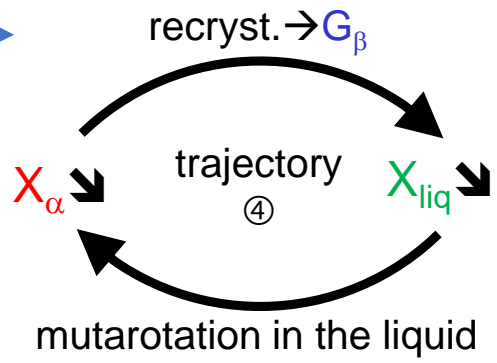| GLUCOSE			
T_m	Heating rate	Technique	References
140°C	0.05 °C/min	DSC	Magon et al. [9]
161°C	20°C /min	DSC	Magon et al. [9]
183°C	1500 °C/min	Hyper DSC	Lee et al. [11]

Figure 1
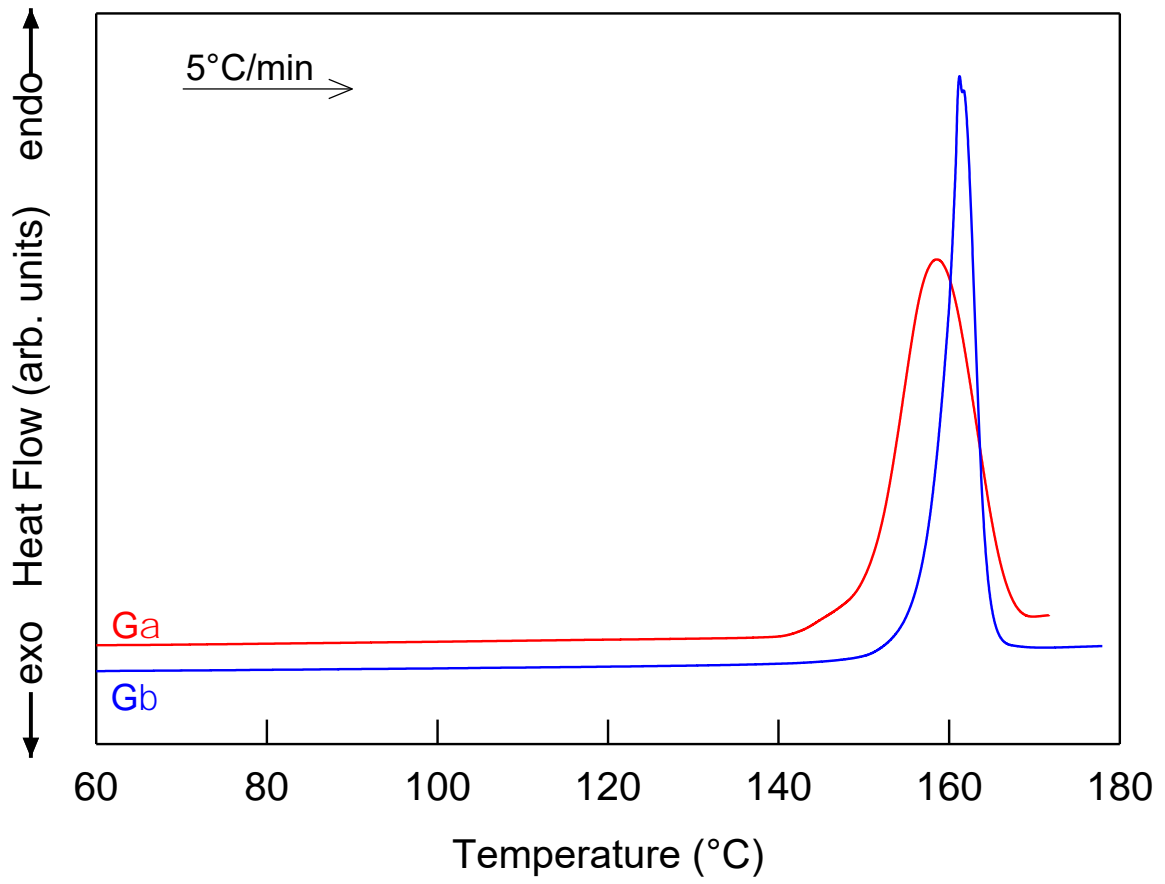
Figure 2
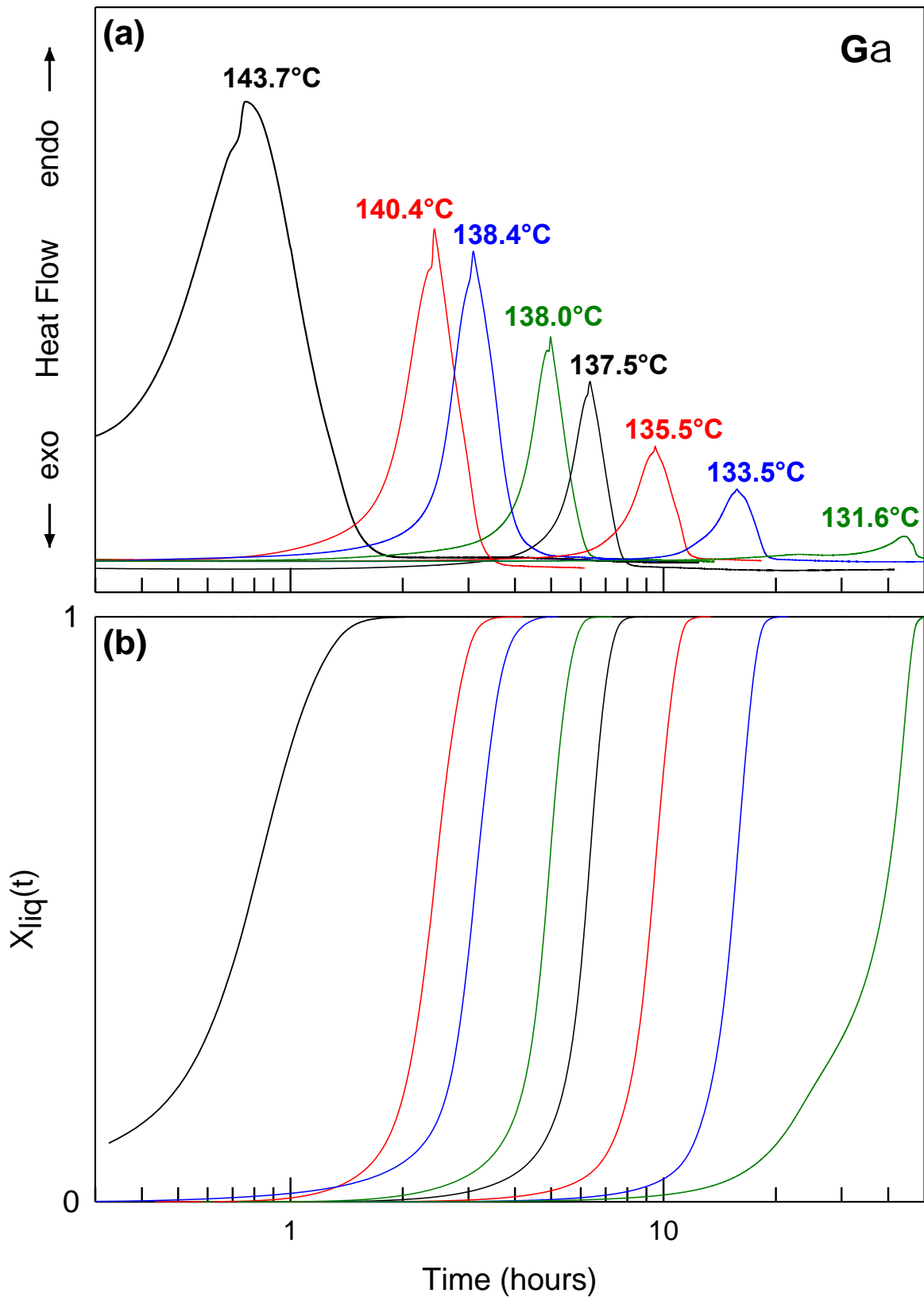
Figure 3
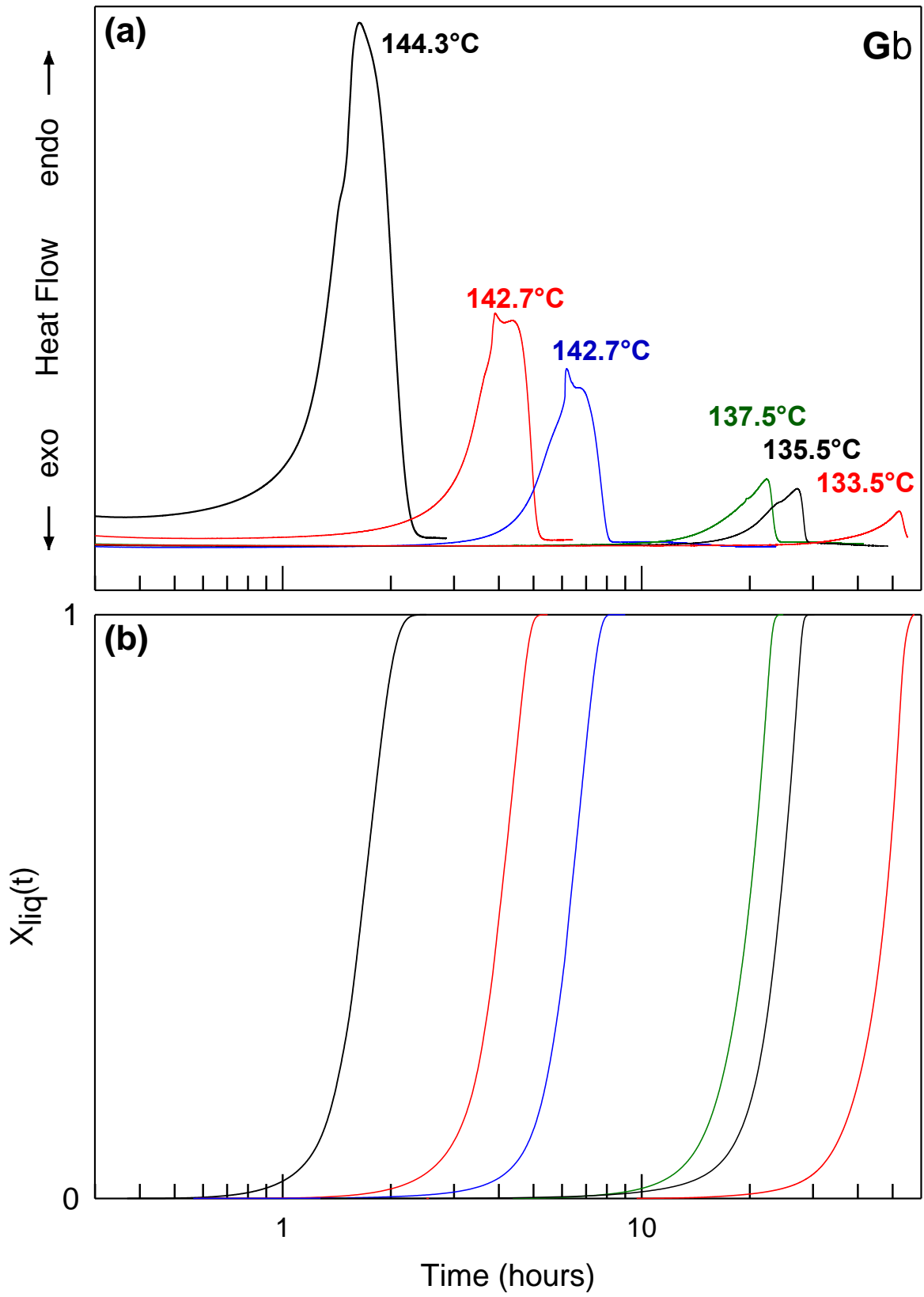
Figure 4
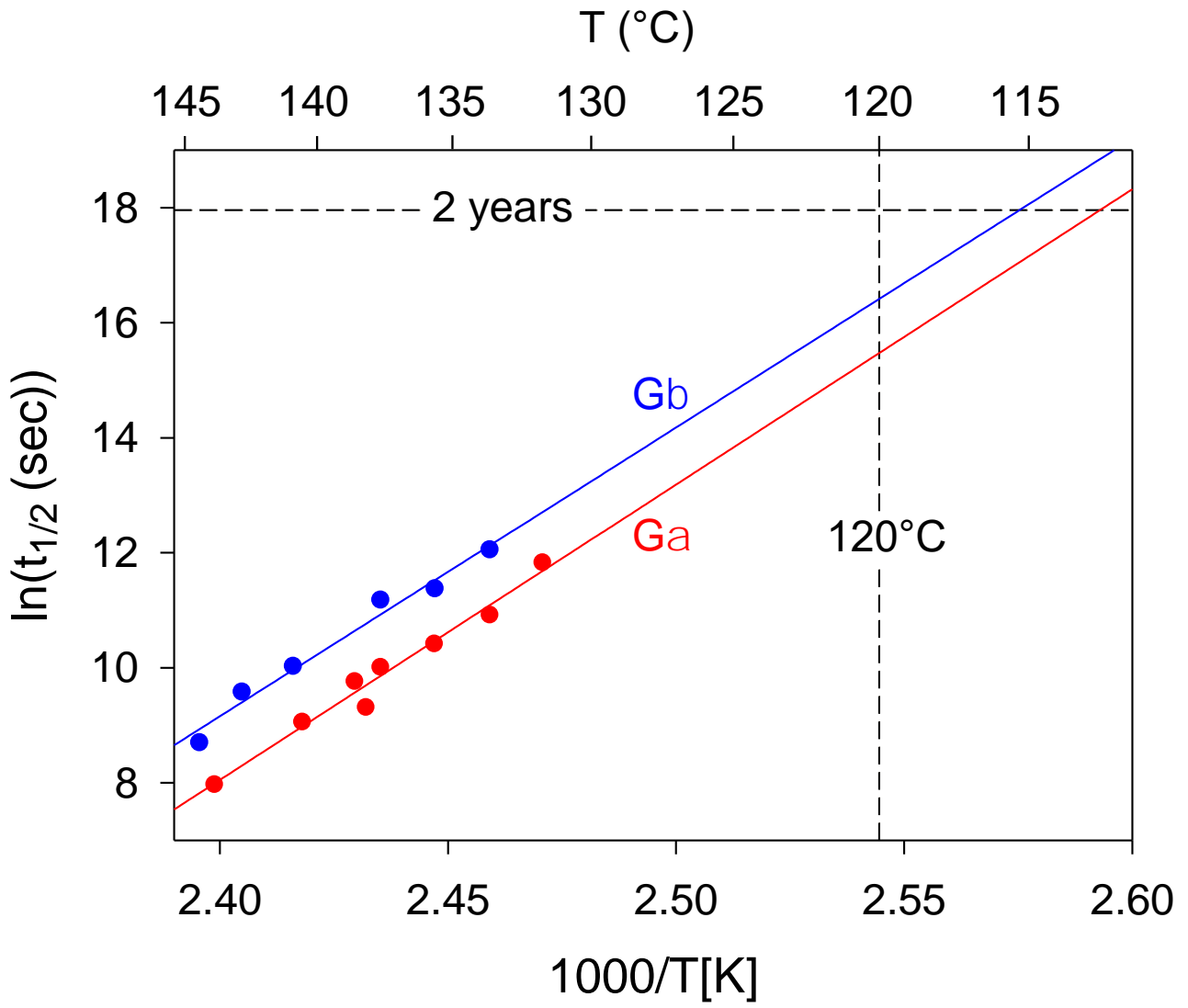
Figure 5

Figure 6

Figure 7

liquefaction of G_β

X_α trajectory ① X_{liq}

mutarotation in the liquid

liquefaction of G_α

X_α trajectory ② X_{liq}

mutarotation in the liquid

liquefaction of G_α

X_α trajectory ④ X_{liq}

mutarotation in the liquid

when G_β liquidus is crossed

recryst.→G_β

X_α trajectory ④ X_{liq}
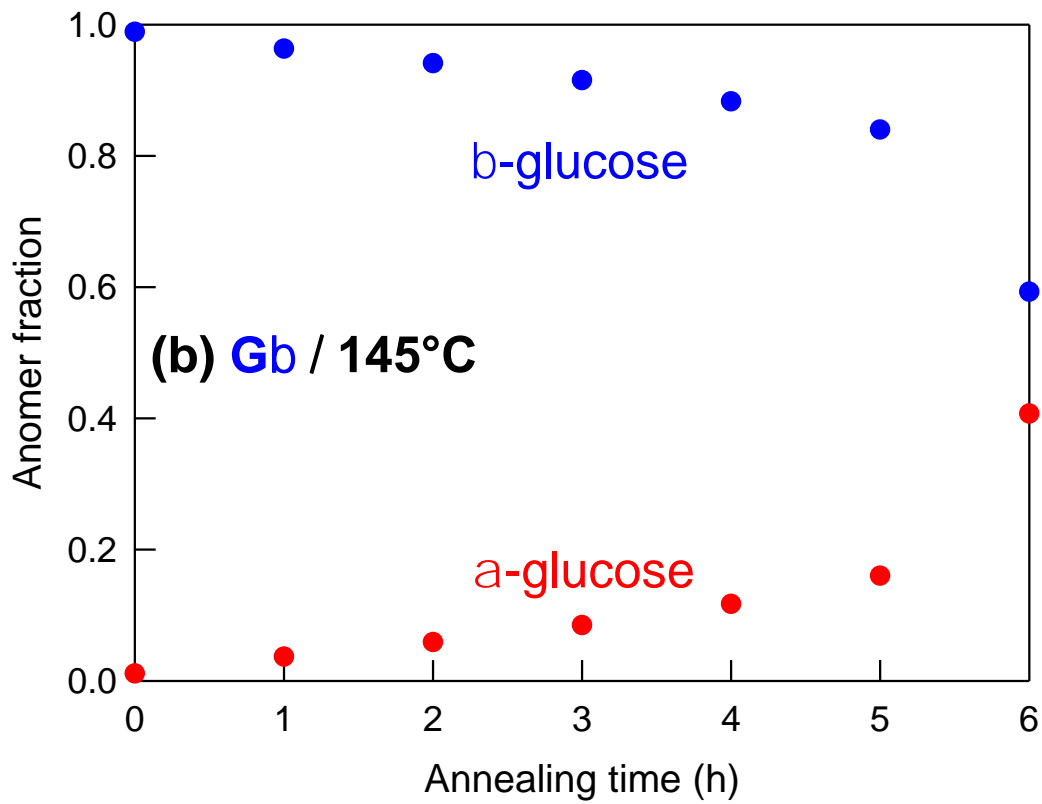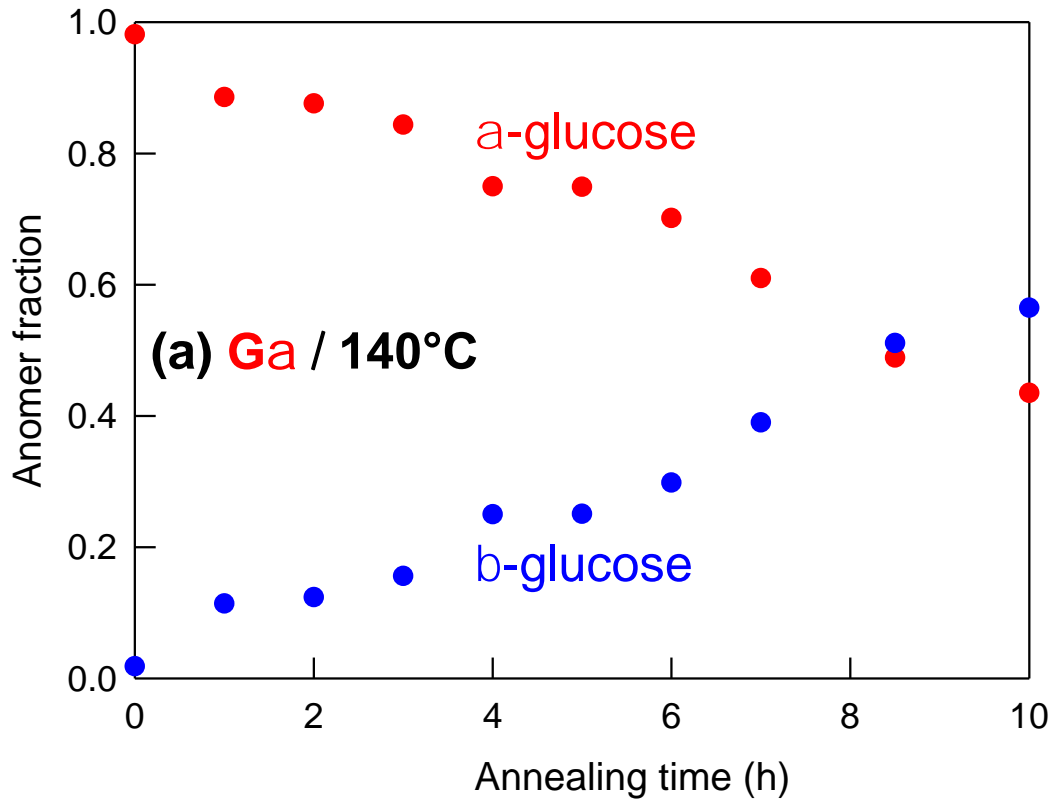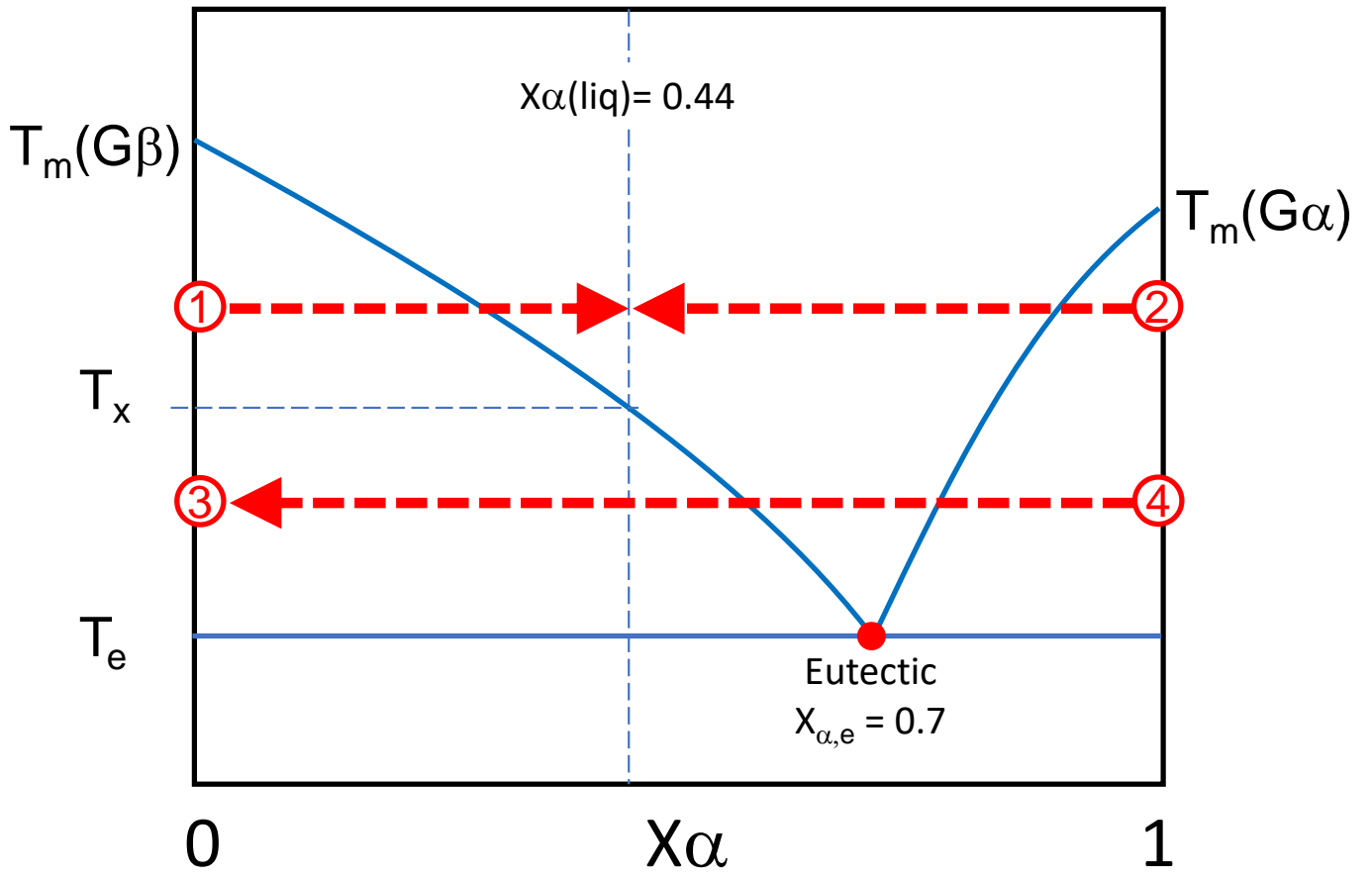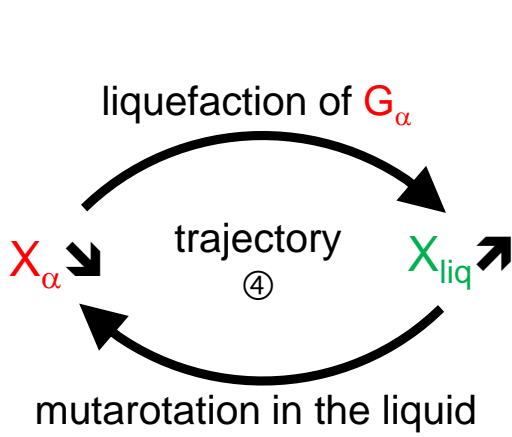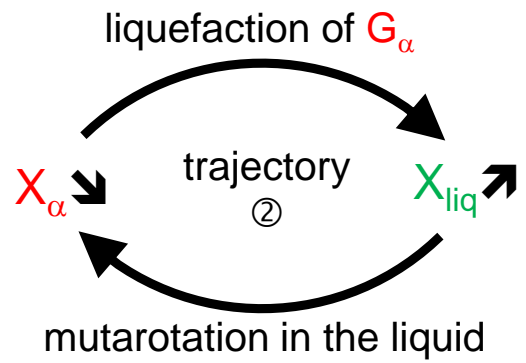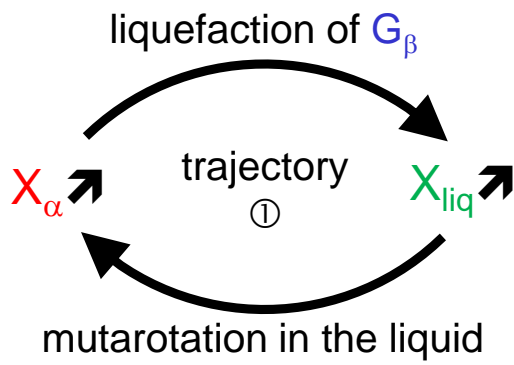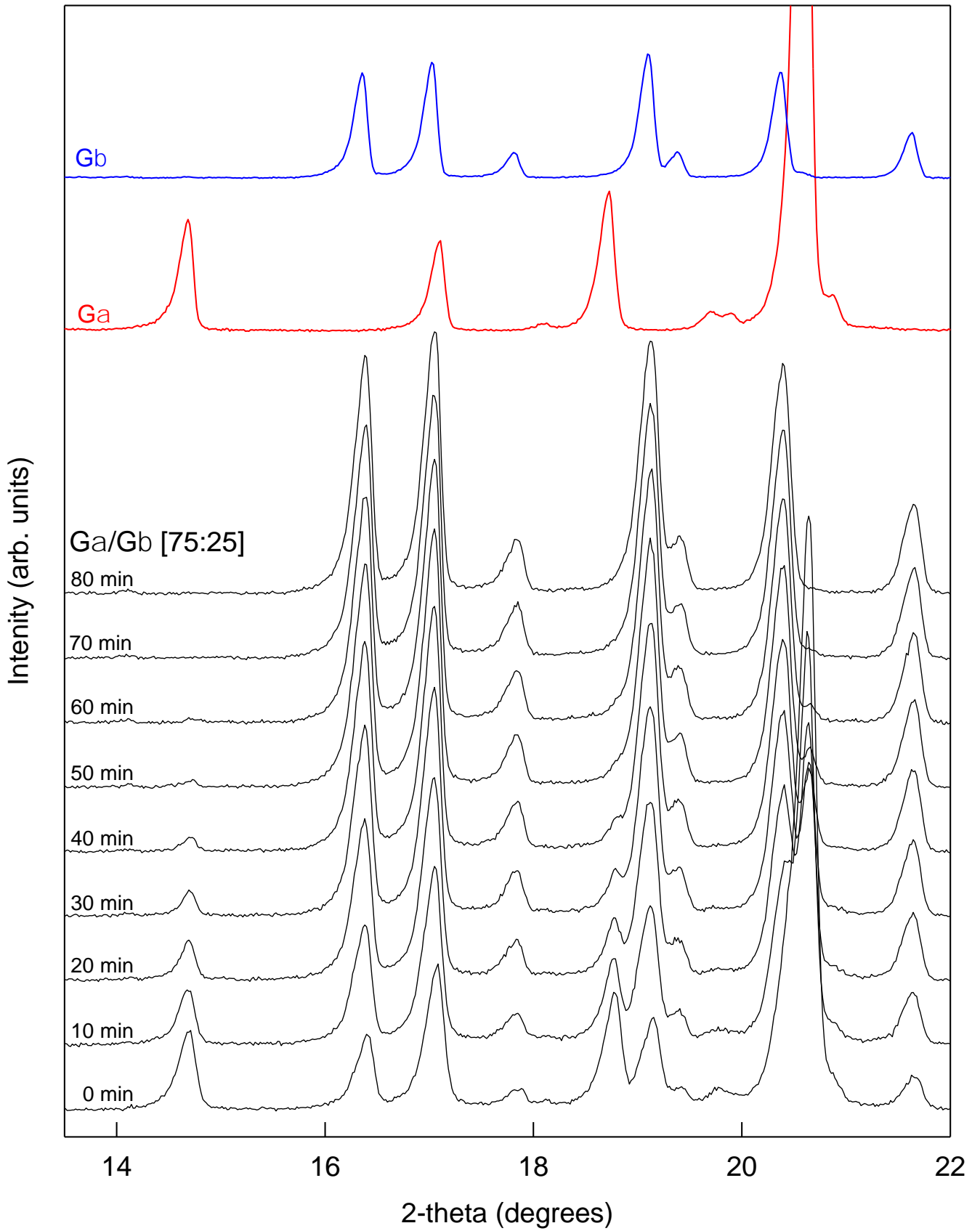
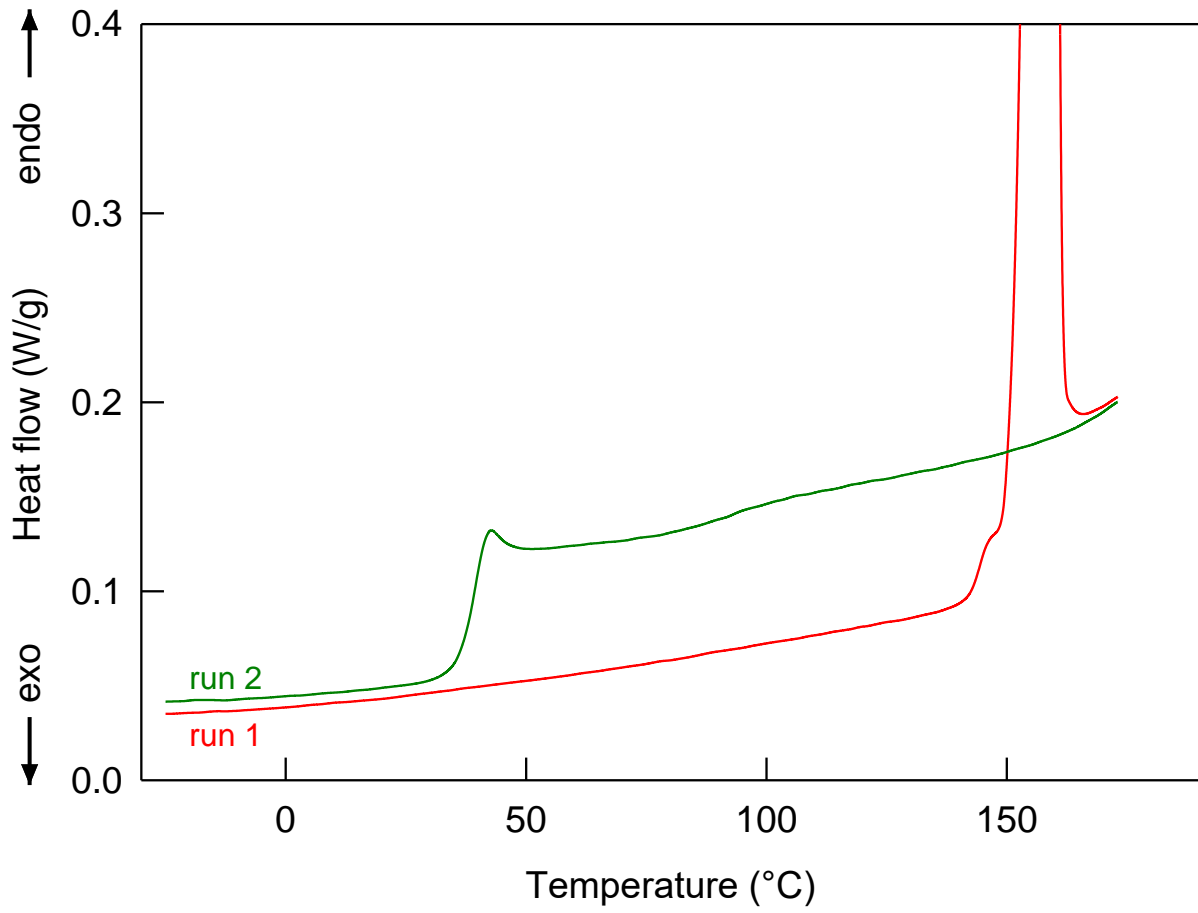mutarotation in the liquid

Figure 8

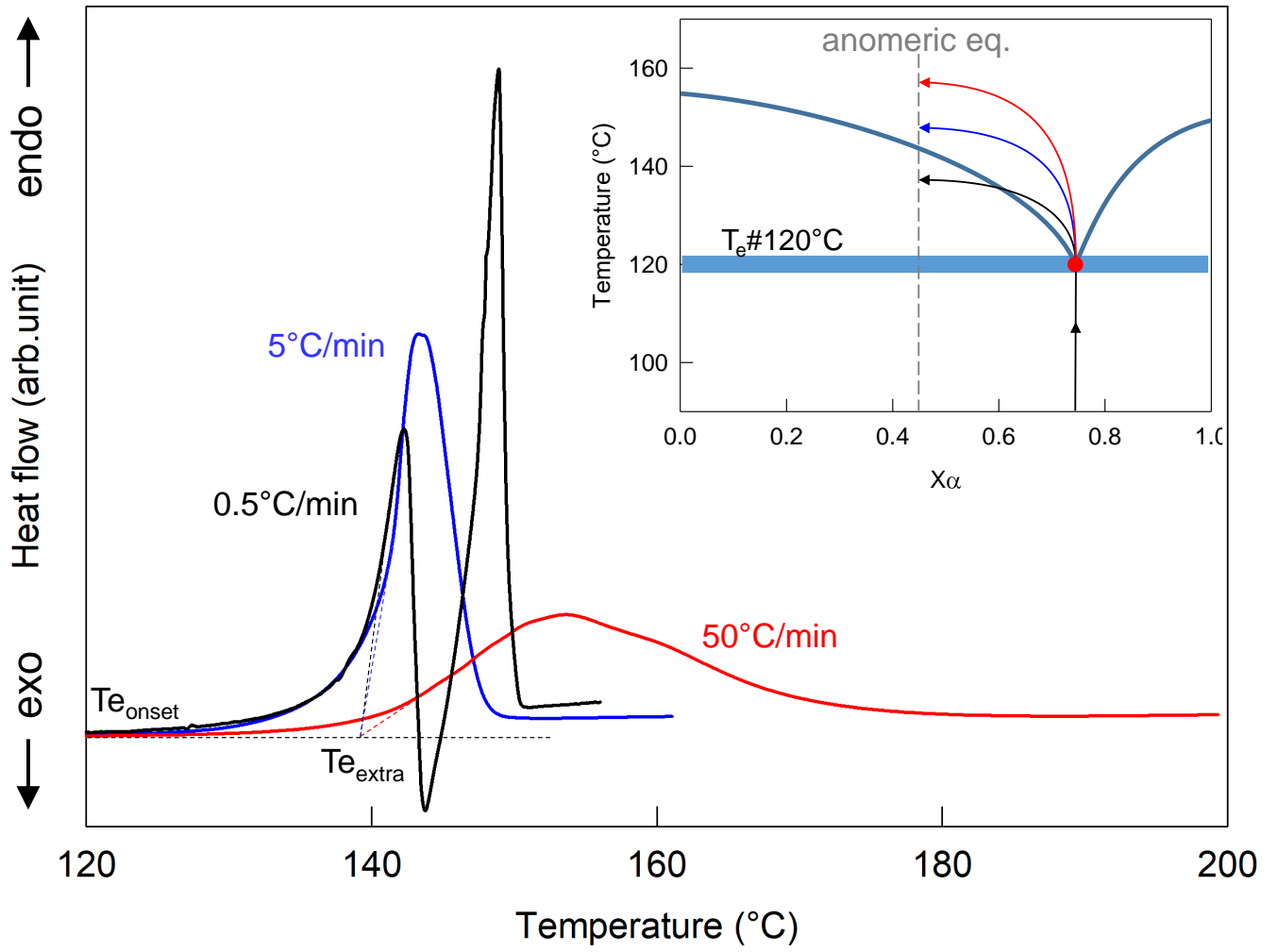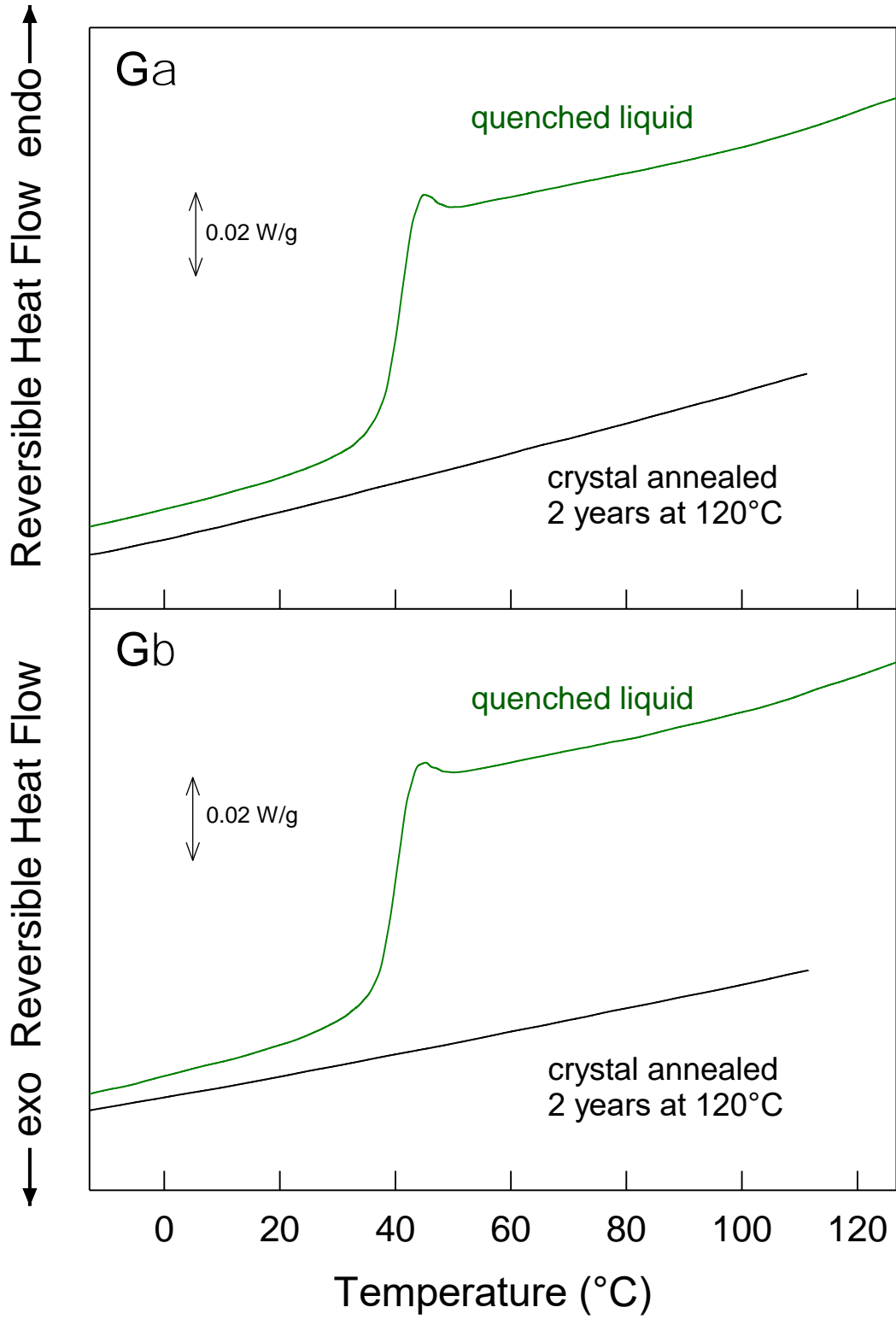Figure 9

Figure 10

Figure 11

REFERENCES

1.   Levine H, Slade L 1992. Another View of Trehalose for Drying and Stabilizing Biological Materials. BioPharm 5:36
2.   Mensink MA, Frijlink HW, van der Voort Maarschalk K, Hinrichs WLJ 2017. How sugars protect proteins in the solid state and during drying (review): Mechanisms of stabilization in relation to stress conditions. European Journal of Pharmaceutics and Biopharmaceutics 114:288-295.(https://doi.org/10.1016/j.ejpb.2017.01.024)
3.   Carpenter JF, Pikal MJ, Chang BS, Randolph TW 1997. Rational Design of Stable Lyophilized Protein Formulations: Some Practical Advice. Pharmaceutical Research 14(8):969-975.(10.1023/A:1012180707283)
4.   Crowe L-M 2002. Lessons from nature: the role of sugars in anhydrobiosis. Comparative Biochemistry and Physiology - Part A: Molecular & Integrative Physiology 131(3):505-513.(10.1016/s1095-6433(01)00503-7)
5.   Taylor LS, Zografi G 1998. Sugar-polymer hydrogen bond interactions in lyophilized amorphous mixtures. Journal of Pharmaceutical Sciences 87(12):1615-1621.(10.1021/js9800174)
6.   Roos Y 1993. Melting and glass transitions of low molecular weight carbohydrates. Carbohydrate Research 238:39-48
7.   Pancoast HM, Junk WR. 1980. Handbook of Sugars. ed.: Avi Publishing Company.
8.   Hurtta M, Pitkanen I, Knuutinen J 2004. Melting behaviour of -sucrose, -glucose and -fructose. Carbohydrate Research 339(13):2267-2273.(10.1016/j.carres.2004.06.022)
9.   Magoń A, Pyda M 2011. Melting, glass transition, and apparent heat capacity of α-d-glucose by thermal analysis. Carbohydrate Research 346(16):2558-2566.(https://doi.org/10.1016/j.carres.2011.08.022)
10.   Magoń A, Pyda M 2013. Apparent heat capacity measurements and thermodynamic functions of d(−)-fructose by standard and temperature-modulated calorimetry. The Journal of Chemical Thermodynamics 56:67-82.(http://doi.org/10.1016/j.jct.2012.07.003)
11.   Lee JW, Thomas LC, Schmidt SJ 2011. Can the Thermodynamic Melting Temperature of Sucrose, Glucose, and Fructose Be Measured Using Rapid-Scanning Differential Scanning Calorimetry (DSC)? Journal of Agricultural and Food Chemistry 59(7):3306-3310.(10.1021/jf104852u)
12.   Roos YH, Franks F, Karel M, Labuza TP, Levine H, Mathlouthi M, Reid D, Shalaev E, Slade L 2012. Comment on the Melting and Decomposition of Sugars. Journal of Agricultural and Food Chemistry 60(41):10359-10362.(10.1021/jf3002526)
13.   Tombari E, Ferrari C, Salvetti G, Johari GP 2007. Spontaneous liquifaction of isomerizable molecular crystals. The Journal of Chemical Physics 126(2):021107.(10.1063/1.2432345)
14.   Wunderlich B 2007. One hundred years research on supercooling and superheating. Thermochimica Acta 461(1):4-13.(https://doi.org/10.1016/j.tca.2006.11.015)
15.   Lee JW, Thomas LC, Jerrell J, Feng H, Cadwallader KR, Schmidt SJ 2011. Investigation of Thermal Decomposition as the Kinetic Process That Causes the Loss of Crystalline Structure in Sucrose Using a Chemical Analysis Approach (Part II). Journal of Agricultural and Food Chemistry 59(2):702-712.(10.1021/jf104235d)
16.   Lee JW, Thomas LC, Schmidt SJ 2011. Investigation of the Heating Rate Dependency Associated with the Loss of Crystalline Structure in Sucrose, Glucose, and Fructose Using a

Thermal Analysis Approach (Part I). Journal of Agricultural and Food Chemistry 59(2):684-701.(10.1021/jf1042344)

17.   Dujardin N, Willart JF, Dudognon E, Danède F, Descamps M 2010. First obtaining of glass solutions and phase diagram of glucose with fully tunable anomeric concentration. Journal of Pharmaceutical Sciences 99(3):1476-1483.(10.1002/jps.21900)

18.   McDonald TRR, Beevers CA 1950. The crystal structure of α-D-glucose. Acta Crystallographica 3:394

19.   Chu SSC, Jeffrey GA 1968. The refinement of the crystal structures of [beta]-d-glucose and cellobiose. Acta Crystallographica Section B 24(6):830-838.(doi:10.1107/S0567740868003250)

20.   McDonald TRR, Beevers CA 1952. The crystal and molecular structure of α–Glucose. Acta Crystallographica 5:654

21.   Ferrier WG 1960. The crystal structure of -D-glucose. Acta Crystallographica

22.   Broido A, Houminer Y, Patai S 1966. Pyrolytic reactions carbohydrates Part1 Mutarotation molten D-glucose. Journal of the Chemical Society B Physical Organic 5:411-414